The Astrophysical Journal, 704:117–125, 2009 October 10 doi:10.1088/0004-637X/704/1/117


# LYMAN BREAK GALAXIES AT $z \sim 5$: REST-FRAME UV SPECTRA. III.*

Hiroki Kajino[1], Kouji Ohta[1], Ikuru Iwata[2], Kiyoto Yabe[1], Suraphong Yuma[1], Masayuki Akiyama[3], Naoyuki Tamura[4], Kentaro Aoki[4], and Marcin Sawicki[5]

[1] Department of Astronomy, Kyoto University, Kyoto 606-8502, Japan; ohta@kusastro.kyoto-u.ac.jp
[2] Okayama Astrophysical Observatory, National Astronomical Observatory of Japan, Okayama 719-0232, Japan
[3] Astronomical Institute, Tohoku University, Sendai 980-77, Japan
[4] Subaru Telescope, National Astronomical Observatory of Japan, 650 North A'ohoku Place, Hilo, HI 96720, USA
[5] Department of Astronomy and Physics, St. Mary's University, 923 Robie St., Halifax, Nova Scotia, B3H 3C3, Canada
*Received 2008 December 26; accepted 2009 August 14; published 2009 September 21*

## ABSTRACT

We present results of optical spectroscopic observations of candidates of Lyman break galaxies (LBGs) at $z \sim 5$ in the region, including the GOODS-N and the J0053+1234 regions by using Gemini Multi-Object Spectrograph North and South, respectively. Among 25 candidates, five objects are identified to be at $z \sim 5$ (two of them were already identified by an earlier study) and one object very close to the color-selection window turned out to be a foreground galaxy. With this spectroscopically identified sample and those from previous studies, we derived the lower limits on the number density of bright ($M_{UV} < -22.0$ mag) LBGs at $z \sim 5$. These lower limits are comparable to or slightly smaller than the number densities of UV luminosity functions (UVLFs) that show the smaller number density among $z \sim 5$ UVLFs in literature. However, by considering that there remain many LBG candidates without spectroscopic observations, the number density of bright LBGs is expected to increase by a factor of two or more. The evidence for the deficiency of UV luminous LBGs with large Ly$\alpha$ equivalent widths was reinforced. We discuss possible causes for the deficiency and prefer the interpretation of dust absorption.

*Key words:* galaxies: evolution – galaxies: formation – galaxies: high-redshift

*Online-only material:* color figures

## 1. INTRODUCTION

To understand the formation and evolution of galaxies, it is necessary to search and study high-redshift galaxies. Lyman break galaxies (LBGs), which are selected by rest-frame UV broadband photometry (e.g., Steidel & Hamilton 1992; Steidel et al. 1995), make the largest sample of galaxies at $z \gtrsim 3$ among various populations selected through different methods, and their statistical and individual studies have been made extensively. For instance, based on photometric samples, the rest-frame UV luminosity functions (UVLFs) of LBGs at $z \sim 3$–6 are derived (e.g., Steidel et al. 1999; Iwata et al. 2003, 2007; Lehnert & Bremer 2003; Ouchi et al. 2004; Beckwith et al. 2006; Sawicki & Thompson 2006; Yoshida et al. 2006; Bouwens et al. 2007) and attempts to measure the LF have been made even at higher redshifts (e.g., Richard et al. 2006, 2008; Stark et al. 2007; Bouwens et al. 2008; Stanway et al. 2008b; Oesch et al. 2008). These studies are revealing the cosmic star-formation history; the cosmic star-formation rate density rises from $z \sim 5$–6 to $z \sim 2$–3 and turns to decline toward $z \sim 0$ (e.g., Hopkins & Beacom 2006). However, two different evolutions of UVLFs are claimed. One is that from $z \sim 5$ to $\sim 3$, the number density of UV faint galaxies increases, while that of bright galaxies remains almost constant (Sawicki & Thompson 2006; Iwata et al. 2007). The other is that while the number density of UV faint galaxies remains constant, that of bright galaxies increases (Yoshida et al. 2006; Bouwens et al. 2007). The number density of UVLF in bright part is key to understanding the galaxy evolution at these redshifts.

Follow-up optical spectroscopic surveys have also been made (e.g., Steidel et al. 1996a, 1996b, 1999). Shapley et al. (2003) studied ~800 spectra of $z \sim 3$ LBGs and classified them into four categories according to their rest-frame Ly$\alpha$ equivalent widths (EWs). They made a composite spectrum of each category and found that LBGs with smaller Ly$\alpha$ EW tend to show larger EWs of low-ionization interstellar (LIS) absorption lines, larger velocity difference between Ly$\alpha$ and LIS absorption, and redder rest-frame UV continua. Follow-up spectroscopic observations have been made for LBGs at $z \gtrsim 5$ (e.g., Lehnert & Bremer 2003; Stanway et al. 2003, 2004, 2007; Ando et al. 2004, 2007; Dow-Hygelund et al. 2005, 2007). As redshift increases, the targets become fainter and the characteristic spectral features move into the wavelength region where night sky emissions are severe; thus, detailed spectroscopic studies of $z \gtrsim 5$ LBGs are still not easy. Hence, the sample size of spectroscopically identified $z \sim 5$ LBGs is still very small. In addition, the spectroscopic studies have so far been relying on the Ly$\alpha$ emission, and the features seen in the continuum are still not clear except for rare bright objects such as gravitationally lensed LBGs (Frye et al. 2002; Swinbank et al. 2007). Thus, a larger deep spectroscopic sample of LBGs at $z \gtrsim 5$ is required to reveal spectroscopic properties of LBGs.

We have constructed a large sample of LBGs at $z \sim 5$ based on Subaru/Suprime-Cam observations (Iwata et al. 2003, 2007), and we are conducting spectroscopic observations of selected targets from the photometric sample. The target fields are the regions including the GOODS-N and the J0053+1234 regions. The total area of the survey fields is 1290 arcmin$^2$ and 228 objects are obtained with $z' < 25.0$ mag, i.e., $L > L^*$ in the UVLF of $z \sim 5$ LBGs (Iwata et al. 2007). The results of our follow-up spectroscopy with Faint Object Camera

* Based on observations obtained at the Gemini Observatory, which is operated by the Association of Universities for Research in Astronomy, Inc., under a cooperative agreement with the National Science Foundation on behalf of the Gemini partnership: the NSF (United States), the Science and Technology Facilities Council (United Kingdom), the National Research Council (Canada), CONICYT (Chile), the Australian Research Council (Australia), Ministério da Ciência e Tecnologia (Brazil), and SECYT (Argentina).

**Table 1**
Journal of Observations

| Gemini ID | Field | Center of Mask R.A. | (J2000.0) Decl. | Instrument | Observation Period | Exposure Time (s) |
|---|---|---|---|---|---|---|
| GN2007A-Q018-02 | GOODS-N | 12:36:20.680 | 62:14:13.00 | GMOS-N | 2007 May 25 to 2007 Jun 10 | 20 × 1800 |
| GN2007A-Q018-04 | Flanking field of GOODS-N | 12:37:51.830 | 62:08:44.00 | GMOS-N | 2007 Jun 17 to 2007 Jun 24 | 16 × 1800 |
| GS2007B-Q206-01 | J0053+1234 | 00:53:26.930 | 12:31:45.00 | GMOS-S | 2007 Oct 5 to 2008 Jan 6 | 31 × 1800 |

And Spectrograph (FOCAS) on the Subaru Telescope were reported by Ando et al. (2004, 2007), and the number of bright ($z' < 25.0$ mag) $z \sim 5$ LBGs with spectroscopic identification was nine, and that of faint ($z' \geqslant 25.0$ mag) LBGs was two. Combining the data with those from literature, Ando et al. (2006) claimed the deficiency of bright LBGs with large EWs of Ly$\alpha$ emissions at $z \sim 5$ and $z \sim 6$. However, the sample size of our spectroscopically confirmed LBGs at $z \sim 5$ was still very small. Thus, we intended to increase the size of the spectroscopic sample.

In this paper, we present the results of spectroscopic observations of $z \sim 5$ LBGs in the region, including the GOODS-N and the J0053+1234 regions with Gemini Multi-Object Spectrograph North (GMOS-N) and South (GMOS-S), respectively. Gemini/GMOS spectrographs have nod-and-shuffle capability, which enables us to subtract sky emission more clearly and helps in the detection of continuum features. In Section 2, we describe our sample selection, observations, and data reduction. The results and obtained spectra are presented in Section 3. In Section 4, we discuss the distribution of redshifts and colors, an implication to the UVLF of LBGs at $z \sim 5$, and rest-frame EWs of Ly$\alpha$ emission, combining present results with previous data by Ando et al. (2004, 2007) and others. Throughout this paper, we used a flat $\Lambda$ cosmology; $\Omega_M = 0.3$, $\Omega_\Lambda = 0.7$, and $H_0 = 70$ km s$^{-1}$ Mpc$^{-1}$. All magnitudes are given in the AB system (Oke & Gunn 1983).

## 2. TARGET SELECTION, OBSERVATIONS, AND DATA REDUCTION

The photometric sample of LBGs at $z \sim 5$ was obtained in the region including the GOODS-N and the J0053+1234 regions, based on $V$-, $I_C$-, and $z'$-band images taken with Subaru/Suprime-Cam (Iwata et al. 2003, 2007). The color criteria for $z \sim 5$ LBGs are

$$V - I_C > 1.55 \quad (1)$$

and

$$V - I_C > 7.0(I_C - z') + 0.15. \quad (2)$$

The sample size in the region, including the GOODS-N region, is ~600 objects ($z' < 26.5$ mag) and ~200 objects ($z' < 25.5$ mag) in the J0053+1234 region. More details of the imaging observations and the color selection are described by Iwata et al. (2007). We selected bright ($z' < 25.0$ mag) $z \sim 5$ LBG candidates as main spectroscopic targets, aiming at detecting the continuum and absorption features. Because the entire survey field is too wide to obtain the spectra of all LBG candidates in the survey field, we selected multi-object spectroscopy (MOS) fields to cover as many main targets as possible. When two slits in the mask design were in conflict, we chose the slit of the object with higher surface brightness. We filled the unused parts of the masks with as many faint ($z' \geqslant 25$ mag) targets as possible. We designed three masks in the GOODS-N, its flanking field, and the J0053+1234 regions. The numbers of bright LBGs in the masks are 7, 5, and 10, respectively, and the numbers of faint objects are 1, 2, and 0, respectively. In the J0053+1234 region, we also observed five objects outside, but near the border of, our color selection criteria in order to examine our color selection criteria.

The preference to the higher surface brightness mentioned above may introduce a bias to the spectroscopic sample. Thus, we examined average surface brightness within $r_{50}$ (50% light encircled radius from SExtractor) as well as concentration parameter ($C = 5 \log(r_{80}/r_{20})$) of the spectroscopic sample among the whole photometric sample in the GOODS-N region, including the samples by Ando et al. (2004, 2007). It is found that in $z' < 25.0$ mag, the spectroscopic sample is fairly chosen from the whole sample, while in $z' > 25.0$ mag the spectroscopic sample tends to bias toward LBGs with the higher average surface brightness and the higher concentration.

Optical spectroscopy was made by using the nod-and-shuffle (micro-shuffle) mode of GMOS (Hook et al. 2004) attached to the 8 m Gemini Telescope North and South. All of the observations were executed in a queue mode during 2007 May–June for the GOODS-N region (Gemini programs GN2007A-Q018-02 and GN2007A-Q018-04) and from 2007 October to 2008 January for the J0053+1234 region (Gemini program GS2007B-Q206-01). We used the R400 grating blazed at 7640 Å with the order cut filter of OG515. The slits of 1″ width and 4″–9″ lengths were used and the spectral resolution was ~8 Å measured from night-sky emission lines. Each spectrum covers the wavelength range of ~5500–10000 Å depending on the slit position on the mask. The exposure time for individual frame was 1800 s, and total exposure times were 10, 8, and 15.5 hr for the GOODS-N, its flanking field, and the J0053+1234 region, respectively. Nod interval for each position was 45 s for all observations, and the nod distances were 3″, 3″, and 1.″4 for the GOODS-N, its flanking field, and the J0053+1234 region, respectively. Seeing sizes were typically about 0.″7 for both the GMOS-N and the GMOS-S regions. The details of observations for each field are listed in Tables 1 and 2.

The data were reduced with the Gemini Image Reduction and Analysis Facility (IRAF)[6] package, standard IRAF packages, and the custom code using the FITSIO package. First, bias subtraction was made with a combined bias frame. Next, we shifted the images with the shuffle distance along the slit and subtracted them from the images before shifting to remove the night-sky emissions. The resultant images were flat-fielded using the dome flat images taken at the time closest

[6] IRAF is distributed by National Optical Astronomical Observatories (NOAO), which is operated by the Association of Universities for Research in Astronomy (AURA), Inc., under cooperative agreement with the NSF.

**Table 2**
Observing Setup

| Gemini ID | Grating | Filter | Slit Size (arcsec × arcsec) | Pixel Scale (Å × arcsec) |
|---|---|---|---|---|
| GN2007A-Q018-02 | R400+_G5305 | OG515_G0306 | 1 × 8 | 2.7 × 0.15 |
| GN2007A-Q018-04 | R400+_G5305 | OG515_G0306 | 1 × 9 | 2.7 × 0.15 |
| GS2007B-Q206-01 | R400+_G5325 | OG515_G0330 | 1 × 3.8 | 1.3 × 0.15 |

**Table 3**
Properties of Identified LBGs

| ID | R.A. (J2000.0) | Decl. (J2000.0) | $z'$ (mag) | $V - I_C$ (mag) | $I_C - z'$ (mag) | $M_{1600}$ (mag) | Redshift | Ly$\alpha$ EW$_{rest}$ (Å) |
|---|---|---|---|---|---|---|---|---|
| N106944 | 12:37:58.12 | 62:09:51.3 | $24.55 \pm 0.05$ | $2.32 \pm 0.10$ | $0.018 \pm 0.045$ | $-21.73 \pm 0.05$ | $4.64 \pm 0.01$ | 0 |
| N127245 | 12:36:35.49 | 62:13:50.3 | $24.89 \pm 0.06$ | $1.96 \pm 0.11$ | $0.072 \pm 0.065$ | $-21.30 \pm 0.06$ | $4.42 \pm 0.01$ | $5.0^{+5.0}_{-1.9}$ |
| N141368 | 12:36:14.21 | 62:16:43.3 | $25.32 \pm 0.13$ | $>2.21$ | $0.212 \pm 0.140$ | $-21.13 \pm 0.13$ | $5.15 \pm 0.01$ | $5.0^{+6.0}_{-2.4}$ |
| S101900 | 00:53:35.57 | 12:31:44.1 | $23.72 \pm 0.02$ | $1.67 \pm 0.02$ | $0.168 \pm 0.014$ | $-22.54 \pm 0.02$ | $4.61 \pm 0.01$ | $18^{+18}_{-8}$ |
| S103759 | 00:53:33.21 | 12:32:07.3 | $23.54 \pm 0.02$ | $2.88 \pm 0.03$ | $0.033 \pm 0.012$ | $-22.80 \pm 0.02$ | $4.82 \pm 0.01$ | $5.1^{+3.4}_{-1.7}$ |

to when the object images were taken. Then, the images were combined after correcting a small offset of the spectra in each exposure. Wavelength calibration was made by using the night-sky emission lines. The accuracy estimated from night-sky emission lines was ∼0.3–0.7 Å. One-dimensional positive and negative spectra were extracted with our custom code, with the aperture determined by eye. We combined the positive and the negative spectra and applied sensitivity correction to them using the spectra of standard stars (Feige 66 for GMOS-N and LTT 9239 for GMOS-S). We did not make a flux calibration. The final spectra were obtained by binning the pixels along the wavelength direction to improve the signal-to-noise ratio (S/N). To have an identical wavelength bin size (13.4 Å), the numbers of pixels binned are 5 and 10 for spectra obtained by GMOS-N and GMOS-S, respectively.

## 3. RESULTS

### 3.1. LBGs Identified to be $z \sim 5$

Among 22 bright LBG candidates, we identified four objects to be LBGs at $z \sim 5$. We also identified one object as a $z = 5.15$ LBG among three faint targets based on its Ly$\alpha$ emission. The resultant spectra of the LBGs identified are shown in Figure 1.

N106944 shows a clear continuum depression and some LIS absorption lines (Si II λ1260, O I+Si II λ1303, and C II λ1335); hence, we can securely conclude that it is at $z \sim 5$. The redshift determined from the LIS absorption lines is $4.64 \pm 0.01$. N127245, S101900, and S103759 show a single emission line and a continuum depression in a wavelength region shortward of the emission line; hence, their identifications are also secure. The redshifts of N127245, S101900, and S103759 determined from the Ly$\alpha$ emission line are $4.42 \pm 0.01$, $4.61 \pm 0.01$, and $4.82 \pm 0.01$, respectively.[7] The other identified LBG, N141368, that is chosen from the faint LBG sample ($z' = 25.32$ mag) shows a single emission line at 7478 Å. If the emission line is [O III]λ5007 or H$\beta$, its redshift is 0.49 or 0.54, respectively. In this case, a strong H$\alpha$ emission line is expected to come at 9803 Å or 10097 Å, respectively. However, no significant emission is seen at this wavelength, though the S/N in such a red region is very low. If the emission line is [O III]λ5007, the [O III]λ4959 should be seen at 7406 Å with a 1/3 flux, which is not seen. Another possibility is an identification of [O II]λ3727. If this is the case, an H$\beta$ emission line should come at 9754 Å. Again no significant emission line is seen. Since the continuum feature longward of the emission line is slightly seen in the wavelength regions where the sky emission is weak and there seems to be a break around at 7460 Å, we identified this emission line as Ly$\alpha$. The redshift determined from the Ly$\alpha$ emission is $5.15 \pm 0.01$. The properties of the LBGs identified are summarized in Table 3.

Among 18 remaining bright LBG candidates, we concluded that one object (N111905) is a foreground contamination as described in Section 3.2. The remaining objects were not identified because of a low S/N in their spectra or no spectral feature in the observed wavelength coverage. Combining with our previous results by Ando et al. (2004, 2007), the total number of our spectroscopic LBG sample is 16.

We examined the identification rates of the spectroscopic sample including the results by Ando et al. (2004, 2007). Targets with the higher average surface brightness tend to be identified efficiently; in $z' < 25$ mag, among targets with an average surface brightness higher than 29.8 mag arcsec$^{-2}$ the identification rate is ∼60%, while it is ∼10% among targets with a fainter average surface brightness. Among targets with $z' < 25$ mag, highly concentrated objects tend to be identified; ∼50% are identified among objects with $C < 2.5$, while only ∼20% are identified those with $C > 2.5$. These trends, however, cannot be seen among targets with $z' > 25$ mag; the identification rate is higher in more extended objects, though the subsample size is smaller. It should be worth mentioning that the identified LBGs with $z' > 25$ mag show strong Ly$\alpha$ emission, while most of the identified LBGs with $z' < 25$ mag show no or very weak Ly$\alpha$ emission. The trend that luminous LBGs do not show strong Ly$\alpha$ emission prevents us from achieving a high-identification rate even in bright LBG sample. The trend and its physical cause will be discussed in Section 4.3.

### 3.2. Foreground Objects

We identified three foreground objects: one is in our color criteria and the others are outside of the criteria. The former (N111905) shows an emission line at 8209 Å and the continuum is seen shortward of the emission line. Thus, this object should be

[7] Two identified LBGs in the J0053+1234 region, S101900 ($z = 4.61$) and S103759 ($z = 4.82$), had been previously identified by Steidel et al. (1999) in their $z \sim 4$ survey, where these were found to be at the upper end of their redshift selection window.

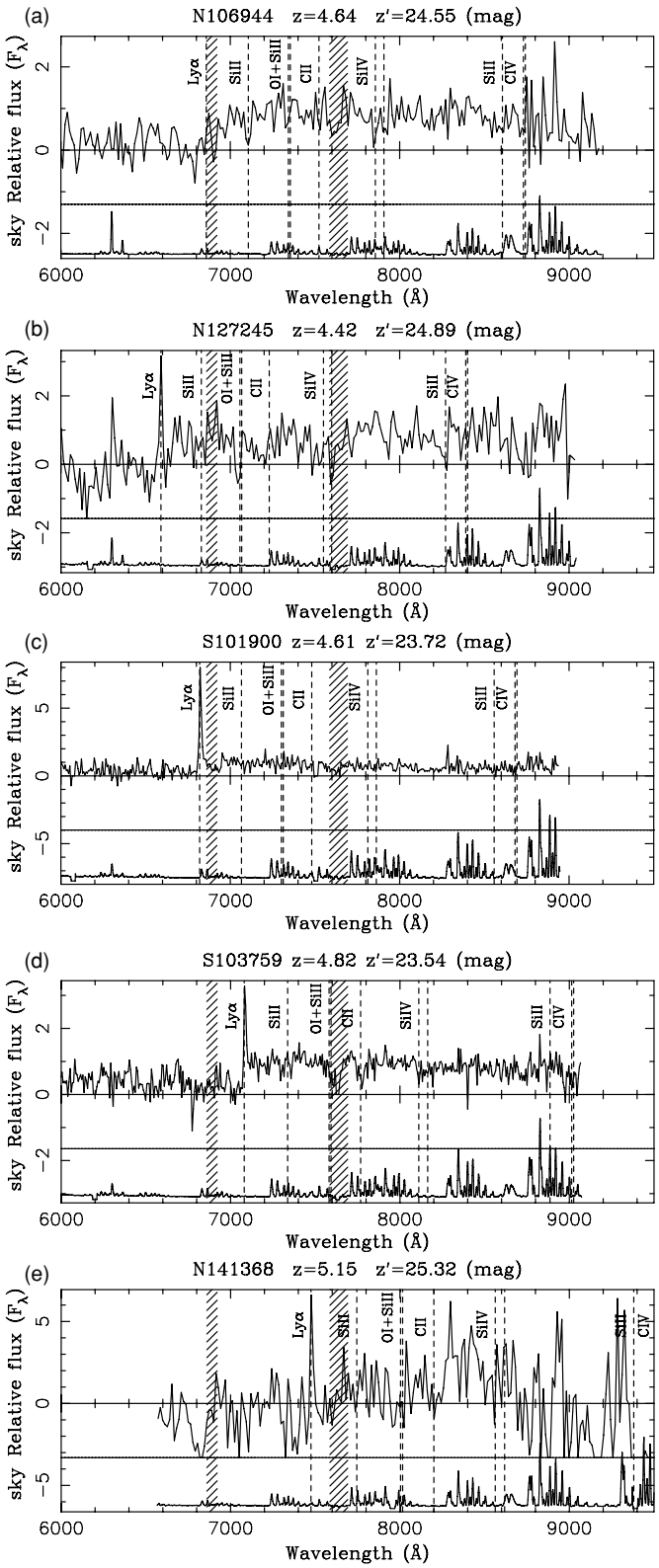


**Figure 1.** Spectrum of observed $z \sim 5$ LBGs identified. (a) N106944. (b) N127245. (c) S101900. (d) S103759. (e) N141368. The positions of redshifted Ly$\alpha$ and interstellar absorption lines are shown with vertical dashed lines. The sky spectrum is shown in the lower part of each panel. The atmospheric A-band and B-band absorptions are shown with vertical hatched regions.

a foreground object. If the emission line at 8209 Å is [O II]$\lambda$3727, its redshift is 1.20, and no other major emission lines seen in star-forming galaxies come into the observed wavelength coverage. If the emission line is one of H$\beta$, [O III]$\lambda$4959, or

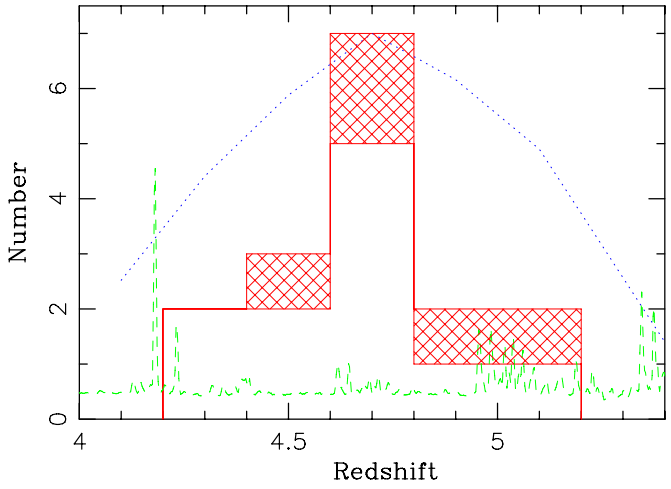


**Figure 2.** Redshift distribution of identified LBGs. The hatched histogram shows the LBGs identified in this study, and the white histogram shows the LBGs from previous studies by Ando et al. (2004, 2007). The dotted line is the normalized expected redshift distribution. The dashed line represents the sky intensity at the redshifted Ly$\alpha$ wavelength.

(A color version of this figure is available in the online journal.)

[O III]$\lambda$5007, other lines should appear around the emission line, but no other emission lines can be seen. Hence, probably the object is a foreground object at $z = 1.20$. However, its $V - I_C$ color is somewhat redder than the expected color for a star-forming galaxy at $z = 1.20$. It is worth noting that the object is located quite close to the selection criteria (see Section 4.1). The contamination rate in our spectroscopic sample with $z'$-band magnitude from 24.0 to 25.0 in the GOODS-N region is 1/9 (including those from Ando et al. 2004, 2007), which is not larger than the estimated value of 17% (Iwata et al. 2007).

One of the five targets outside of the color selection window is identified to be a Galactic M star. Its $V - I_C$ and $I_C - z'$ colors are consistent with typical colors of Galactic M stars (see Section 4.1). Another object outside of the color selection window is identified to be an elliptical galaxy at $z = 0.39$. Its spectrum clearly shows an Mgb absorption, 4000 Å break, and Ca H and K absorptions. No emission lines are seen. However, its $V - I_C$ and $I_C - z'$ colors are somewhat bluer than the expected colors for an early-type galaxy at $z = 0.39$. The remaining objects were not identified because of low S/N in their spectra or no spectral feature in the observed wavelength coverage.

## 4. DISCUSSION

### *4.1. Redshift and Color Distribution of $z \sim 5$ LBGs*

Figure 2 shows the redshift distribution of spectroscopically confirmed $z \sim 5$ LBGs in this study and that by Ando et al. (2004, 2007). The hatched and white histograms show $z \sim 5$ LBGs from the present results and the FOCAS sample by Ando et al. (2004, 2007), respectively. We show the expected redshift distribution of our sample of $z \sim 5$ LBGs by a dotted line normalized at $z = 4.7$. The expected distribution was calculated based on the detection rates of the LBGs against the apparent magnitude and the redshift for each survey field by considering the survey volume and reached depth in UVLF at each redshift bin (Ando et al. 2007). We also plotted the intensity of night-sky emission at the wavelength corresponding to the redshifted Ly$\alpha$. Although the observed redshift distribution seems to be concentrated at $z = 4.7$, it is consistent with the expected distribution within the statistical uncertainty.

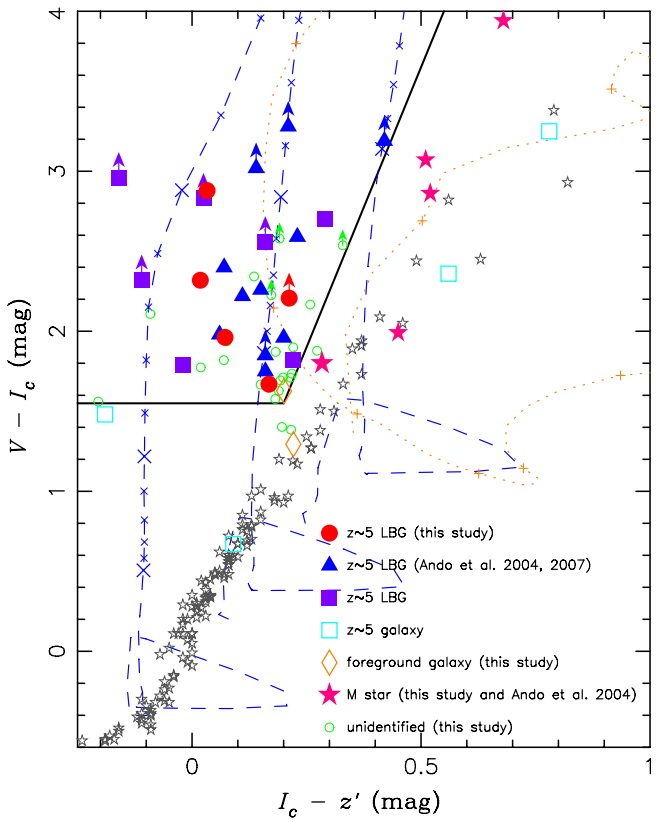


**Figure 3.** $V - I_C$ vs. $I_C - z'$ diagram. Filled circles show spectroscopically identified LBGs in this study. Filled triangles show the LBGs by Ando et al. (2004, 2007). Open diamonds show the foreground galaxies found in this study. Filled stars show the Galactic stars in this study and those by Ando et al. (2004). Small open circles represent LBG candidates unidentified in this study. Filled squares refer to LBGs which are detected by Iwata et al. (2007) and spectroscopically identified by other studies (Spinrad et al. 1998; Steidel et al. 1999; Dawson et al. 2001, 2002; Fernández-Soto et al. 2001; Barger et al. 2008). Open squares refer to spectroscopically identified $z \sim 5$ galaxies (Stern & Spinrad 1999; Dawson et al. 2001; Cowie et al. 2004) but not in the color criteria. The solid line shows our selection color criteria (Equations (1) and (2)). Dashed lines show the model color tracks of star-forming galaxies from Iwata et al. (2007), with $E(B - V) = 0.0$, 0.4, and 0.8 mag from left to right, respectively (see text for details). Small crosses are plotted on the tracks for $z \geqslant 4.0$ with a redshift interval of 0.1. Symbols at $z = 4.0$, 4.5, and 5.0 are enlarged. The dotted line represents the color track of an early-type galaxy (Coleman et al. 1980). Small pluses are plotted on the track with a redshift interval of 0.5. Small open stars represent colors of Galactic A0-M9 stars calculated from the library by Pickles (1998).

(A color version of this figure is available in the online journal.)

Figure 3 shows the positions of the observed LBGs in the two-color ($V - I_C$ and $I_C - z'$) diagram. A solid line shows our color selection criteria represented by Equations (1) and (2) (Iwata et al. 2007). The filled circles and the filled triangles show the LBGs observed in this study and those of Ando et al. (2004, 2007), respectively. The open diamonds show the foreground galaxies found in this study. The filled stars show the Galactic stars in this study and those of Ando et al. (2004). The small open circles show LBG candidates unidentified in this study. The three dashed tracks show model colors of star-forming galaxies. The model spectrum of a star-forming galaxy is calculated with PÈGASE version 2 (Fioc & Rocca-Volmerange 1997), by assuming a constant star-formation history with an age of 100 Myr, Salpeter initial mass function (IMF; Salpeter 1955) with upper mass of 120 $M_\odot$ and lower mass of 0.1 $M_\odot$, and the dust extinction curve by Calzetti et al. (2000). Average IGM attenuation is calculated based on a prescription by Inoue et al. (2005). Three tracks represent models of $E(B - V)$ of 0.0, 0.4, and 0.8 mag. A dotted line represents a color track of an early-type galaxy (Coleman et al. 1980). As mentioned in Section 3.2, one foreground galaxy resides in the color selection window, but it is very close to the boundary of the window. While the majority of the spectroscopically confirmed $z \sim 5$ LBGs lie away from the boundary, unidentified objects are close to it.

In Figure 3, $z \sim 5$ galaxies spectroscopically identified by other studies in the survey fields (Tables 3 and 4 of Iwata et al. 2007; Barger et al. 2008) are also plotted. Filled and open squares show the identified objects in the color selection window and outside it, respectively. The properties of all spectroscopically identified objects at $z \geqslant 4.2$ are listed in Tables 4 and 5. Among them, one object shows peculiar colors of $I_C - z' \sim 0.1$ mag and $V - I_C \sim 0.7$ mag. Iwata et al. (2007) suggest that this object may be a foreground object because the original identification was based on a single emission line. Other two objects with red $I_C - z'$ colors may be dust reddened star-forming galaxies. However, if the redness of these objects is really due to the dust extinction, the extinction at rest-frame 1600 Å corresponds to 8 mag or more and the intrinsic luminosity is huge, if we assume the Calzetti extinction curve. In addition, their $V - I_C$ colors are not consistent with their redshifts; $V - I_C$ colors are too blue to be at $z \sim 5$. These may imply that the spectral models we adopt do not cover the whole real spectra of $z \sim 5$ galaxies. Since we did not take spectra of objects outside of the color criteria extensively, more studies on such galaxies are desirable to know their nature and fraction.

### *4.2. Implications to the UV Luminosity Function of LBGs at $z \sim 5$*

Using the photometric sample, Iwata et al. (2007) derived the UVLF of LBGs at $z \sim 5$ in the region, including the GOODS-N and the J0053+1234 regions. They found that there is a significant population of bright ($M_{UV} < -22.0$ mag) LBGs at $z \sim 5$ comparable to that of $z \sim 3$–4, while the faint ($M_{UV} > -21.0$ mag) end of their UVLF shows a gradual increase from $z \sim 5$ to $z \sim 3$ (Sawicki & Thompson 2006). So Iwata et al. (2007) suggest luminosity dependent evolution of LBGs at these redshifts. However, different results are derived from other studies of UVLF of LBGs at $z \sim 5$. The UVLFs in Subaru Deep Field and Subaru/XMM-Newton Deep Field derived by Ouchi et al. (2004) and Yoshida et al. (2006) show a smaller number density of bright LBGs than that found by Iwata et al. (2003, 2007), and suggest an evolution of the number density in the bright part of the UVLF from $z \sim 5$ to $z \sim 3$. The UVLFs by Beckwith et al. (2006) and Bouwens et al. (2007) also show a similar trend to those by Ouchi et al. (2004) and Yoshida et al. (2006). The difference between the number density of bright ($M_{UV} < -22.0$ mag) LBGs of Iwata et al. (2003, 2007) and that of Ouchi et al. (2004) and Yoshida et al. (2006) is 0.5–1.0 dex.

The cause of the divergence of UVLFs is still unknown. Field-to-field variance may exist, or different filter sets used in various LBG surveys may cause the difference (Stanway et al. 2008a). The spectroscopic sample helps to constrain the UVLF. We derived the lower limit of the number density of LBGs at $z \sim 5$ in the GOODS-N and the J0053+1234 regions, using the spectroscopically confirmed LBGs, including the spectroscopy from the literature (Dawson et al. 2001, 2002; Fernández-Soto et al. 2001; Spinrad et al. 1998; Steidel et al. 1999; Barger et al. 2008), but not including $z \sim 5$ galaxies outside the color selection window. We derived the lower limits for each

**Table 4**
Spectroscopically Identified LBGs in the Sample by Iwata et al. (2007)

| ID | R.A. (J2000.0) | Decl. (J2000.0) | $z'$ (mag) | $V - I_C$ (mag) | $I_C - z'$ (mag) | Redshift | Reference[a] |
|---|---|---|---|---|---|---|---|
| N146624(F36279-1750) | 12:36:27.74 | +62:17:47.8 | 26.05 | >2.32 | −0.11 | 4.94 | 1 |
| N119188(HDF 3-951.0) | 12:37:00.23 | +62:12:19.8 | 24.69 | 1.82 | 0.22 | 5.34 | 2 |
| N116886(HDF 4-625.0) | 12:36:44.65 | +62:11:50.7 | 25.24 | >2.87 | 0.03 | 4.58 | 3 |
| N136110(ES1) | 12:36:49.23 | +62:15:38.8 | 25.48 | >2.96 | −0.16 | 5.19 | 4 |
| N135557 | 12:36:55.48 | +62:15:32.9 | 25.64 | >2.56 | 0.16 | 5.19 | 5 |
| N139345 | 12:38:06.84 | +62:16:20.4 | 24.89 | 1.79 | −0.02 | 4.91 | 5 |
| N104268(A04-1) | 12:38:11.32 | +62:09:19.4 | 24.02 | 2.22 | 0.11 | 4.52 | 6 |
| N144200(A04-2) | 12:37:57.49 | +62:17:19.0 | 24.08 | 2.40 | 0.07 | 4.70 | 6 |
| N95819(A04-4) | 12:37:05.68 | +62:07:43.3 | 24.50 | 2.26 | 0.15 | 4.65 | 6 |
| N139294(A04-5) | 12:38:28.96 | +62:16:18.8 | 24.39 | 1.96 | 0.20 | 4.67 | 6 |
| N149472(A04-6) | 12:38:25.52 | +62:18:19.7 | 24.87 | >3.02 | 0.14 | 4.86 | 6 |
| N129178(A04-7) | 12:38:04.36 | +62:14:19.7 | 24.29 | >3.28 | 0.21 | 5.18 | 6 |
| N148198(A04-8) | 12:38:16.63 | +62:18:05.3 | 24.50 | >3.19 | 0.42 | 4.62 | 6 |
| N106944 | 12:37:58.13 | +62:09:51.3 | 24.55 | 2.32 | 0.02 | 4.64 | 7 |
| N127245 | 12:36:35.49 | +62:13:50.3 | 24.89 | 1.96 | 0.07 | 4.42 | 7 |
| N141368 | 12:36:14.21 | +62:16:43.3 | 25.32 | >2.21 | 0.21 | 5.15 | 7 |
| S64032(CDFb-G05) | 00:53:51.28 | +12:24:21.3 | 24.31 | 2.70 | 0.29 | 4.49 | 8 |
| S106426(A06-1) | 00:52:21.34 | +12:32:35.3 | 24.07 | 2.59 | 0.23 | 4.80 | 6 |
| S104115(A06-2) | 00:52:43.27 | +12:32:08.2 | 24.22 | 1.75 | 0.16 | 4.27 | 6 |
| S091813(A06-3) | 00:52:39.88 | +12:29:44.1 | 25.03 | 1.98 | 0.06 | 4.39 | 6 |
| S093014(A06-4) | 00:52:37.37 | +12:29:58.7 | 25.26 | >1.85 | 0.16 | 4.49 | 6 |
| S101900(CDFa-GD7) | 00:53:35.57 | +12:31:44.1 | 23.72 | 1.67 | 0.17 | 4.61 | 7 |
| S103759(CDFa-G1) | 00:53:33.21 | +12:32:07.3 | 23.54 | 2.88 | 0.03 | 4.82 | 7 |

**Note.**
[a] 1. Dawson et al. 2001; 2. Spinrad et al. 1998; 3. Fernández-Soto et al. 2001; 4. Dawson et al. 2002; 5. Barger et al. 2008; 6. Ando et al. 2004, 2007; 7. This study; 8. Steidel et al. 1999.

**Table 5**
Spectroscopically Identified Galaxies ($z > 4.2$) Out of the Color Selection by Iwata et al. (2007)

| ID | R.A. (J2000.0) | Decl. (J2000.0) | $z'$ (mag) | $V - I_C$ (mag) | $I_C - z'$ (mag) | Redshift | Reference[a] |
|---|---|---|---|---|---|---|---|
| F36219-1516 | 12:36:21.88 | +62:15:17.0 | 25.39 | 0.67 | 0.09 | 4.89 | 1 |
| F36376-1453 | 12:36:37.62 | +62:14:53.8 | 21.97 | 3.25 | 0.78 | 4.89 | 1 |
| HDF 4-439.0 | 12:36:43.84 | +62:12:41.7 | 25.29 | 1.48 | −0.19 | 4.54 | 2 |
| GOODS J123721.03+621502.1 | 12:37:21.00 | +62:15:02.1 | 23.32 | 2.36 | 0.56 | 4.76 | 3 |

**Note.**
[a] 1. Dawson et al. 2001; 2. Stern & Spinrad 1999; 3. Cowie et al. 2004.

field by dividing the numbers of spectroscopically confirmed LBGs by the effective volume in each magnitude bin from Iwata et al. (2007). Then we averaged the lower limits of two fields weighting with their survey areas. When we calculate the UV absolute magnitude of the spectroscopic sample, we used the fixed redshift of $z = 4.8$ for consistency with the estimation of the effective volume. The difference between the UV absolute magnitude by this assumption and that from spectroscopic redshift is $\lesssim$0.2 mag.

Figure 4 shows the derived lower limits on the number density of LBGs at $z \sim 5$ in the GOODS-N region, the J0053+1234 region, and their average. The solid and the dashed line shows the Schechter function fit to the UVLF of Iwata et al. (2007) and Yoshida et al. (2006), respectively with the data points (small crosses and pluses, respectively). The conservative estimation of the lower limits by using only the spectroscopic sample gives the number density of LBGs comparable to that by Yoshida et al. (2006) in the magnitude range of $23.5 < z' < 24.0$ mag and a slightly smaller value in $24.0 < z' < 24.5$ mag. The fractions of spectroscopically confirmed LBGs to the total photometric sample in the magnitude range of $23.5 < z' < 24.0$ mag, $24.0 < z' < 24.5$ mag, $24.5 < z' < 25.0$ mag, and $25.0 < z' < 25.5$ mag are 0/5, 5/35, 6/72, and 3/126, respectively in the GOODS-N, and 2/10, 3/22, 0/79, and 2/122, respectively in the J0053+1234 region. Considering that more than half of the photometric sample by Iwata et al. (2007) are not observed yet, the number density of LBGs in each magnitude bin is expected to be larger than this lower limit by a factor of two or more and approach toward the values of Iwata et al. (2007). We estimated the expected number densities if the full photometric sample were spectroscopically observed, by multiplying the number of the photometric sample by the success rate of spectroscopy in each magnitude bin, and by dividing it by the effective volume from Iwata et al. (2007). Results are shown with arrows in Figure 4. The expected number densities of bright ($M_{UV} < -22.0$ mag) LBGs are comparable to or slightly larger than those by Yoshida et al. (2006). Since we regarded all unidentified objects as foreground objects in this estimation, true number densities are probably larger than these estimations. Thus, the number densities in the bright part from the spectroscopic sample are still consistent with those from Iwata et al. (2003, 2007).

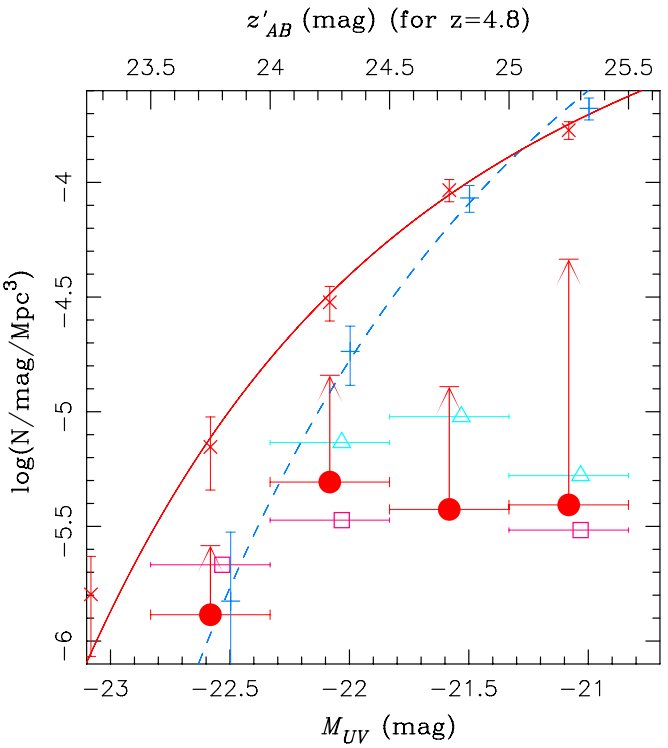


**Figure 4.** Lower limits on the number density of LBGs at $z \sim 5$. Open triangles, open squares, and filled circles show the lower limits on UVLF in the GOODS-N region, the J0053+1234 region, and the average of them, respectively. The data points of lower limits in each field are shifted +0.05 mag for clarity. Vertical arrows show the expected values derived by multiplying the number of photometric sample by the success rate of the spectroscopic sample in this study and that by Ando et al. (2004, 2007). Note that unidentified objects are not included in the lower limits. The solid and the dashed lines show the Schechter function fit to the UVLF by Iwata et al. (2007) and Yoshida et al. (2006), respectively with the data points (small crosses and pluses, respectively).

(A color version of this figure is available in the online journal.)

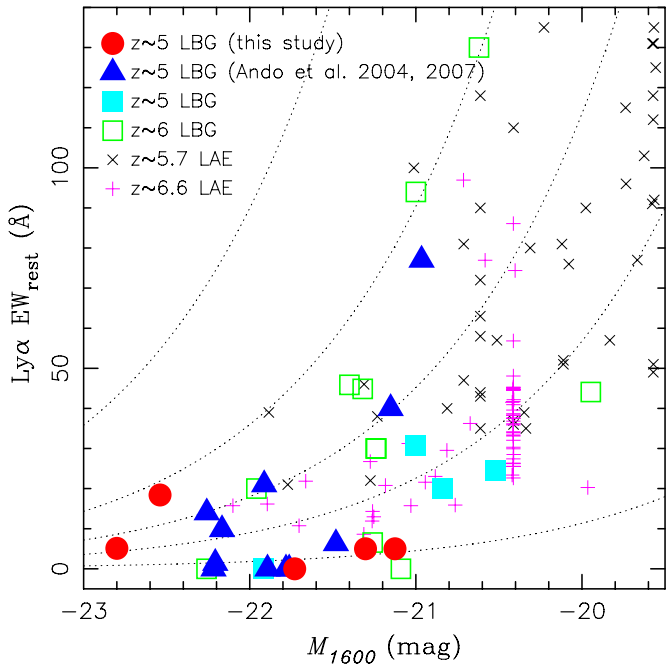


**Figure 5.** Rest-frame EWs of Ly$\alpha$ emission against absolute magnitude at rest frame 1600 Å for galaxies at $z \sim 5$ and $z \sim 6$. Filled circles and filled triangles show our spectroscopic $z \sim 5$ LBGs in this study and those by Ando et al. (2004, 2007), respectively. The other symbols show LBGs and LAEs from the literature. Filled squares, open squares, filled triangles, and open triangles represent $z \sim 5$ LBGs (Lehnert & Bremer 2003; Stanway et al. 2007), $z \sim 6$ LBGs (Lehnert & Bremer 2003; Stanway et al. 2003, 2004, 2007; Nagao et al. 2004, 2005; Dow-Hygelund et al. 2005, 2007), $z \sim 5.7$ LAEs (Ajiki et al. 2003; Shimasaku et al. 2006), and $z \sim 6.6$ LAEs (Taniguchi et al. 2005), respectively. We used the EWs spectroscopically derived for a part of the sample of Taniguchi et al. (2005). Dotted lines show constant Ly$\alpha$ luminosities of $5 \times 10^{43}$, $2 \times 10^{43}$, $10^{43}$, $5 \times 10^{42}$, and $10^{42}$ erg s$^{-1}$ from top left to bottom right.

(A color version of this figure is available in the online journal.)

### *4.3. Rest-frame UV Luminosity and Ly$\alpha$ EW*

Ando et al. (2006) reported the absence of rest-frame UV luminous LBGs with large EW of Ly$\alpha$ emission at $z \sim 5$. Combining recent results of Stanway et al. (2007) and Dow-Hygelund et al. (2007), we update the plot of rest-frame Ly$\alpha$ EW against rest-frame UV absolute magnitude and show it in Figure 5. The rest-frame UV absolute magnitudes of the LBGs and LAEs were calculated from their $z'$-band magnitudes. We chose UV absolute magnitude at 1600 Å ($M_{1600}$) to minimize the effect of uncertainty of the continuum slope. We selected $\beta = -2$ ($f_\lambda \propto \lambda^\beta$) as a typical value for a young starburst. The value of $\beta = -2$ is consistent with the observed $I_C - z'$ colors of spectroscopically confirmed LBGs. The uncertainty of $M_{1600}$ due to the assumption of $\beta$ ($\beta = -2 \pm 1$) is about 0.1–0.2 mag. If the continuum flux densities at longward of Ly$\alpha$ line are listed in the literature, we used them to derive the rest-frame UV absolute magnitudes to mitigate the influence by strong Ly$\alpha$ emission and IGM attenuation in the band (Nagao et al. 2004, 2005; Taniguchi et al. 2005). Filled circles and filled triangles show spectroscopically confirmed $z \sim 5$ LBGs in this study and that by Ando et al. (2004, 2007), respectively. Other symbols show LBGs and LAEs from the literature. The filled squares, open squares, crosses, and pluses represent $z \sim 5$ LBGs (Lehnert & Bremer 2003; Stanway et al. 2007), $z \sim 6$ LBGs (Lehnert & Bremer 2003; Stanway et al. 2003, 2004, 2007; Nagao et al. 2004, 2005; Dow-Hygelund et al. 2005, 2007), $z \sim 5.7$ LAEs (Ajiki et al. 2003; Shimasaku et al. 2006), and $z \sim 6.6$ LAEs (Taniguchi et al. 2005), respectively.

The deficiency of UV luminous LBGs with large Ly$\alpha$ EW is seen in our revised plot. There are no luminous ($M_{1600} < -21.5$ mag) $z \sim 5$ LBGs with large ($> 20$ Å) EW Ly$\alpha$ emission. Although we may miss the faint LBGs with small Ly$\alpha$ EW, we can detect luminous LBGs with large Ly$\alpha$ EW. Thus, the deficiency must be real. Such distribution is also seen among $z \sim 6$ LBGs, $z \sim 5.7$ LAEs, and $z \sim 6.6$ LAEs. The threshold UV magnitude seems to lie around $-21.5$ mag $< M_{1600} < -21.0$ mag, and this value is close to $M_*$ of our $z \sim 5$ LBG sample ($M_* = -21.28$ mag; Iwata et al. 2007). A similar trend can be seen among $z \sim 3$ LBGs (Shapley et al. 2003); a composite spectrum of UV luminous LBGs shows smaller Ly$\alpha$ EW than that of UV faint ones.

The deficiency of UV luminous LBGs with large Ly$\alpha$ EW may reflect the deficiency of LBGs (and LAEs) with large Ly$\alpha$ luminosity. Dotted lines in Figure 5 represent constant Ly$\alpha$ luminosities of $5 \times 10^{43}$, $2 \times 10^{43}$, $10^{43}$, $5 \times 10^{42}$, and $10^{42}$ erg s$^{-1}$ from top left to bottom right. It appears that a very few objects show Ly$\alpha$ luminosity larger than $2 \times 10^{43}$ erg s$^{-1}$. Since the number density of galaxies with such a large Ly$\alpha$ luminosity is small, the deficiency may be due to poor statistics (e.g., Nilsson et al. 2009). Meanwhile, galaxies under constant star formation with ages of 10–100 Myr are expected to show EWs of 100–200 Å intrinsically. (We used the PÈGASE version 2 (Fioc & Rocca-Volmerange 1997), with Salpeter IMF (Salpeter 1955)

with an upper-mass limit of 120 $M_{\odot}$, and assumed the case B recombination and all Lyman continuum photons ionize neutral hydrogen.) Thus, the deficiency of large Ly$\alpha$ EWs among UV luminous ($M_{1600} < -21.5$) galaxies is still mysterious. Possible causes of small EWs in UV luminous LBGs (except for the poor statistics) are (1) difference of escape fraction of Ly$\alpha$ emission; Ly$\alpha$ emission is selectively quenched by dust extinction and/or scattering by neutral hydrogen in more UV luminous galaxies, (2) difference of time scale of star formation; the UV continuum is the probe of star formation with longer time scale than the nebular emission lines, and star-formation age is larger in more UV luminous galaxies, and (3) difference of IMF in the galaxies; deficiency of massive stars in more UV luminous galaxies.

The escape of Ly$\alpha$ emission is a complex problem, and it is thought to depend on the geometry, dynamics, column density, and dust content of neutral hydrogen in/around the star-forming regions. In nearby starburst galaxies, the existence or absence of outflow of neutral hydrogen largely affects the escape fraction, and the effect of dust content is small (e.g., Kunth et al. 1998; Mas-Hesse et al. 2003; Atek et al. 2008). These authors showed that starburst galaxies with static interstellar media show Ly$\alpha$ as absorption, whereas galaxies showing velocity offset between interstellar absorption lines and Ly$\alpha$ show Ly$\alpha$ as emission lines. In high redshift galaxies, on the other hand, $z \sim 3$ LBGs with larger velocity offset between interstellar absorption and Ly$\alpha$ tend to show smaller Ly$\alpha$ EW (Shapley et al. 2003). In addition, $z \sim 3$ LBGs with a large Ly$\alpha$ EW show bluer UV continua (Shapley et al. 2003; Tapken et al. 2007), suggesting that the dust extinction is the main cause for the Ly$\alpha$ quench. At $z \sim 5$, although the correlation between the EW and $I_C - z'$ color is not clear, the LBGs with large Ly$\alpha$ EW (> 40 Å) in our sample and that by Ando et al. (2004, 2007) (combined sample) show relatively blue observed $I_C - z'$ colors ($I_C - z' \sim 0.06$ mag and 0.16 mag). The LBG with the largest EW in the combined sample shows weak or no LIS absorption lines in its UV continuum. We roughly estimated the metallicity of nine $z \sim 5$ LBGs which show LIS absorption lines in the combined sample, using the empirical relation between the metallicity and the EWs of LIS absorption lines (Heckman et al. 1998). The average value is 12+log[O/H] = 7.7 ($\sim 1/10\ Z_{\odot}$; Allende Prieto et al. 2001), suggesting that LBGs at $z \sim 5$ are chemically evolved to some extent and expected to contain dust. These prefer the dust extinction as the major cause for the Ly$\alpha$ quench. If more UV luminous LBGs are more chemically evolved than UV faint ones on average, it suggests that UV luminous LBGs formed earlier (Ando et al. 2006; Iwata et al. 2007). It should be mentioned, however, that color excesses of a part of the photometric LBG sample (Iwata et al. 2007) are derived by spectral energy distribution (SED) fitting by covering rest-frame UV to optical wavelength (Yabe et al. 2009; they assumed the constant star-formation history, the Calzetti extinction curve, and 0.2 solar abundance as a fiducial model), and no clear correlation is seen between the derived color excesses and Ly$\alpha$ EWs. However, the number of LBGs for which both color excesses and spectra are obtained is only five, and the range of the EW is very limited (up to only ~5 Å). We further examined the relation between the $z'$ magnitude and the color excess obtained by SED fitting by Yabe et al. (2009), but found no clear trend.

The age of a galaxy also affects the EW of Ly$\alpha$. Young starbursts are expected to show large Ly$\alpha$ EW, while old galaxies show small EW. The ages of a part of our LBG sample are also obtained by SED fitting (Yabe et al. 2009); no clear relation between the age and the Ly$\alpha$ EW can be seen (the sample size is five as mentioned above). We further examined the distribution of ages against $z'$ magnitude by using results of the SED fitting (Yabe et al. 2009). The derived ages range from a few Myr to a few 100 Myr with a median of 25 Myr under constant star formation, and an absence of young ages (<10 Myr) is seen among bright LBGs ($z' < 25$ mag). However, with the supposed IMF (Salpeter IMF with an upper-mass limit of 100 $M_{\odot}$) in the SED fitting, the Ly$\alpha$ EW is ~100 Å at ages from 10 Myr to 1 Gyr; thus, the age is unlikely to be the primary cause for the small Ly$\alpha$ EW. If we assume an exponentially decaying star-formation history, the EW decreases more rapidly. Since Yabe et al. (2009) also studied the exponentially decaying models with $\tau = 1$ Myr, 10 Myr, 100 Myr, and 1 Gyr, we examined the cases using their data and found that the UV bright LBGs show relatively young ages of 1–10 Myr with a median $\tau$ of ~1 Myr. With these ages, the exponentially decaying model with $\tau = 1$ Myr shows Ly$\alpha$ EWs larger than ~20 Å, again suggesting that the age is not the primary cause for the deficiency of large Ly$\alpha$ EWs. It is worth noting here that for the $z \sim 3$ LBGs, Shapley et al. (2003) claim that the composite spectrum of old LBGs (>1 Gyr) shows larger EW of Ly$\alpha$ emission than young LBGs (< 35 Myr). Shapley et al. (2003) interpret that dust extinction in old LBGs is smaller than in young LBGs that are under active star formation.

A top-heavy IMF produces a large Ly$\alpha$ EW; in less UV luminous $z \sim 5$ galaxies this may occur especially in LAEs. The Salpeter IMF with an upper-mass limit of 120 $M_{\odot}$ produces more than 100 Å of Ly$\alpha$ EW in a young phase (10–100 Myr) under constant star formation and the Case B assumptions as described before. To reduce the EW in the young phase to less than 20–40 Å by changing an upper-mass limit, it should be smaller. If the upper-mass limit is 14–15 $M_{\odot}$, the EW is smaller than ~20 Å at ages larger than 1 Myr. Although this seems to be unlikely for most UV-luminous class active star-forming galaxies at high redshifts, we cannot rule out this possibility completely.

## 5. SUMMARY

We presented the results of optical spectroscopic observations of $z \sim 5$ LBGs. The observations were made in the GOODS-N, its flanking field with GMOS-N, and the J0053+1234 regions with GMOS-S. Of the 25 observed LBG candidates, the number of bright ($z' < 25.0$ mag) LBG candidates is 22. We identified four LBGs among 22 bright targets (two LBGs identified in the J0053+1234 region were already spectroscopically identified by Steidel et al. 1999) and one LBG among three faint targets. The redshift distribution of identified LBGs is consistent with the expected redshift distribution. One target that turned out to be a foreground galaxy is located almost at the boundary of the color selection window in the two-color diagram. The foreground contamination fraction is consistent with model expectations based on simulations (Iwata et al. 2007). At the same time, two objects just outside of the color selection window are identified to be foreground objects: one is an M-type star and the other is an elliptical galaxy at $z = 0.39$.

Using the full spectroscopically confirmed sample, we derived the raw lower limits on the number density of bright ($M_{UV} < -22.0$ mag) LBGs at $z \sim 5$. The lower limits are comparable to or slightly smaller than the number densities derived by Yoshida et al. (2006). However, considering that there remains a number of LBG candidates without spectroscopic

observations, the number density of spectroscopically derived bright LBGs is expected to increase by a factor of two or more.

We confirmed the deficiency of rest-UV luminous ($M_{1600} < -21.5$) LBGs with large rest-frame EW ($> 20$ Å) of Ly$\alpha$ emission (Ando et al. 2006). We discussed possible causes for the deficiency and prefer the interpretation of dust absorption rather than gas outflow, age difference, and IMF difference.

We would like to thank staff members at Gemini observatory for carrying out our observations. Especially, we are grateful to support scientists Atsuko Nitta and Bryan Miller for their helpful comments during preparation. This work was partly made based on Gemini–Subaru machine time exchange program. This work is supported by Grant-in-Aid for Scientific Research on Priority Area (19047003) from the Ministry of Education, Culture, Sports, Science, and Technology of Japan and in part supported by funding from the Natural Sciences and Engineering Research Council of Canada and the Canadian Space Agency.

*Note added in proof.* After submitting the paper, Vanzella et al. (2009) published the results of spectroscopic observations of LBGs at $z \sim 4$, 5, and 6 in the GOODS-South Field, where they also found the trend that UV luminous LBGs do not show strong Ly$\alpha$ emission lines with a larger sample and discussed the possible causes of the trend.

## REFERENCES

Ajiki, M., et al. 2003, AJ, 126, 2091
Allende Prieto, C., Lambert, D. L., & Asplund, M. 2001, ApJ, 556, L63
Ando, M., Ohta, K., Iwata, I., Akiyama, M., Aoki, K., & Tamura, N. 2006, ApJ, 645, L9
Ando, M., Ohta, K., Iwata, I., Akiyama, M., Aoki, K., & Tamura, N. 2007, PASJ, 59, 717
Ando, M., Ohta, K., Iwata, I., Watanabe, C., Tamura, N., Akiyama, M., & Aoki, K. 2004, ApJ, 610, 635
Atek, H., Kunth, D., Hayes, M., Ö-Stlin, G., & Mas-Hesse, J. M. 2008, A&A, 488, 491
Barger, A. J., Cowie, L. L., & Wang, W.-H. 2008, ApJ, 689, 687
Beckwith, S. V. M., et al. 2006, AJ, 132, 1729
Bouwens, R. J., Illingworth, G. D., Franx, M., & Ford, H. 2007, ApJ, 670, 928
Bouwens, R. J., Illingworth, G. D., Franx, M., & Ford, H. 2008, ApJ, 686, 230
Calzetti, D., Armus, L., Bohlin, R. C., Kinney, A. L., Koornneef, J., & Storchi-Bergmann, T. 2000, ApJ, 533, 682
Coleman, G. D., Wu, C.-C., & Weedmann, D. W. 1980, ApJS, 43, 393
Cowie, L. L., Barger, A. J., Hu, E. M., Capak, P., & Songaila, A. 2004, AJ, 127, 3137
Dawson, S., Spinrad, H., Stern, D., Dey, A., van Breugel, W., de Vries, W., & Reuland, M. 2002, ApJ, 570, 92
Dawson, S., Stern, D., Bunker, A. J., Spinrad, H., & Dey, A. 2001, AJ, 122, 598
Dow-Hygelund, C. C., et al. 2005, ApJ, 630, L137
Dow-Hygelund, C. C., et al. 2007, ApJ, 660, 47
Fernández-Soto, A., Lanzetta, K. M., Chen, H.-W., Pascarelle, S. M., & Yahata, N. 2001, ApJS, 135, 41
Fioc, M., & Rocca-Volmerange, B. 1997, A&A, 326, 950
Frye, B., Broadhurst, T., & Benitez, N. 2002, ApJ, 568, 558
Heckman, T. M., Robert, C., Leitherer, C., Garnett, D. R., & van der Rydt, F. 1998, ApJ, 503, 646
Hook, I. M., Jorgensen, I., Allington-Smith, J. R., Davies, R. L., Metcalfe, N., Murowinski, R. G., & Crampton, D. 2004, PASP, 116, 425
Hopkins, A. M., & Beacom, J. F. 2006, ApJ, 651, 142
Inoue, A. K., Iwata, I., Deharveng, J.-M., Buat, V., & Burgarella, D. 2005, A&A, 435, 471
Iwata, I., Ohta, K., Tamura, N., Akiyama, M., Aoki, K., Ando, M., Kiuchi, G., & Sawicki, M. 2007, MNRAS, 376, 1557
Iwata, I., Ohta, K., Tamura, N., Ando, M., Wada, S., Watanabe, C., Akiyama, M., & Aoki, K. 2003, PASJ, 55, 415
Kunth, D., Mas-Hesse, J. M., Terlevich, E., Terlevich, R., Lequeux, J., & Fall, S. M. 1998, A&A, 334, 11
Lehnert, M. D., & Bremer, M. 2003, ApJ, 593, L630
Mas-Hesse, J. M., Kunth, D., Tenorio-Tagle, G., Leitherer, C., Terlevich, R. J., & Terlevich, E. 2003, ApJ, 598, 858
Nagao, T., et al. 2004, ApJ, 613, L9
Nagao, T., et al. 2005, ApJ, 634, 142
Nilsson, K. K., Möller-Nilsson, O., Møller, P., Fynbo, J. P. U., & Shapley, A. E. 2009, MNRAS, in press (arXiv:0907.3733)
Oesch, P. A., et al. 2008, ApJ, in press (arXiv:0804.4874)
Oke, J. B., & Gunn, J. E. 1983, ApJ, 266, 713
Ouchi, M., et al. 2004, ApJ, 611, 660
Pickles, A. J. 1998, PASP, 110, 863
Richard, J., Pelló, R., Schaerer, D., Le Borgne, J.-F., & Kneib, J.-P. 2006, A&A, 456, 861
Richard, J., Stark, D. P., Ellis, R. S., George, M. R., Egami, E., Kneib, J.-P., & Smith, G. P. 2008, ApJ, 685, 705
Salpeter, E. E. 1955, ApJ, 121, 161
Sawicki, M., & Thompson, D. 2006, ApJ, 642, 653
Shapley, A. E., Steidel, C. C., Pettini, M., & Adelberger, K. L. 2003, ApJ, 588, 65
Shimasaku, K., et al. 2006, PASJ, 58, 313
Spinrad, H., Stern, D., Bunker, A. J., Dey, A., Lanzetta, K., Yahil, A., Pascarelle, S., & Fernandez-Soto, A. 1998, AJ, 116, 2617
Stanway, E. R., Bremer, M. N., & Lehnert, M. D. 2008a, MNRAS, 385, 493
Stanway, E. R., Bremer, M. N., Squitieri, V., Douglas, L. S., & Lehnert, M. D. 2008b, MNRAS, 386, 370
Stanway, E. R., Bunker, A. J., & McMahon, R. G. 2003, MNRAS, 342, 439
Stanway, E. R., Bunker, A. J., McMahon, R. G., Ellis, R. S., Treu, T., & McCarthy, P. J. 2004, ApJ, 607, 704
Stanway, E. R., et al. 2007, MNRAS, 376, 727
Stark, D. P., Ellis, R. S., Richard, J., Kneib, J.-P., Smith, G. P., & Santos, M. R. 2007, ApJ, 663, 10
Steidel, C. C., Adelberger, K. L., Giavalisco, M., Dickinson, M., & Pettini, M. 1999, ApJ, 519, 1
Steidel, C. C., Giavalisco, M., Dickinson, M., & Adelberger, K. L. 1996a, AJ, 112, 352
Steidel, C. C., Giavalisco, M., Pettini, M., Dickinson, M., & Adelberger, K. L. 1996b, ApJ, 462, L17
Steidel, C. C., & Hamilton, D 1992, AJ, 104, 941
Steidel, C. C., Pettini, M., & Hamilton, D. 1995, AJ, 110, 2519
Stern, D., & Spinrad, H. 1999, PASP, 111, 1475
Swinbank, A. M., Bower, R. G., Smith, G. P., Wilman, R. J., Smail, I., Ellis, R. S., Morris, S. L., & Kneib, J.-P. 2007, MNRAS, 376, 479
Taniguchi, Y., et al. 2005, PASJ, 57, 165
Tapken, C., Appenzeller, I., Noll, S., Richling, S., Heidt, J., Meinkohn, E., & Mehlert, D. 2007, A&A, 467, 63
Vanzella, E., et al. 2009, ApJ, 695, 1163
Yabe, K., Ohta, K., Iwata, I., Sawicki, M., Tamura, N., Akiyama, M., & Aoki, K. 2009, ApJ, 693, 507
Yoshida, M., et al. 2006, ApJ, 653, 988